

Development of An Assist Upper Limb Exoskeleton For Manual Handling Task

Zefeng Yan, Haoyuan Yi, Zihao Du, Tiantian Huang, Bin Han*, Lufeng Zhang, Ansi Peng and Xinyu Wu*

Abstract—In this paper we describe the construction of a wearable upper arm exoskeleton to provide support for industrial workers who engaged in repetitive handling tasks and patients who full or partial loss of function in their upper limb due to accident injuries, spinal cord and strokes. We use flexible rope driven by a motor to realize the shoulder and elbow joints linkage, use ball screw to realize the self-locking in any position to providing assist for users. This novel design not only saves energy but also make the whole system portable. The total weight of the prototype is only 2 kg. The exoskeleton is connected upper limb with 3 bandages, and users take about 30 seconds to put it on and 20 seconds to put the exoskeleton off without any help. The PD adaptive control method is applied to the proposed exoskeleton to track expected trajectories. Five healthy people participated in data acquisition. Upper limb muscle integrated electromyography (IEMG) of the deltoid muscle(DM), the biceps femoris muscle (BFM), the femoral muscle (FM), the femoral wrist flexor (FWF) were compared in continuous handling for four different loads (0, 1.5, 3, 4.5kg). The average assistance efficiency were 39.1%, 41.5%, 36.5% and 40.6% for the DM, BFM, FM and FWF respectively. The experimental data show that the upper limb exoskeleton can provide assist for workers and protect their upper limbs injuries in long-term handling task.

Index Terms—Upper limb exoskeleton; Muscular activity; IEMG; Adaptive control.

I. Introduction

In the modern manufacturing company, there is still a lot of work that requires manual handling, such as logistics handling, pipeline handling and healthcare[1].

*This work is partially supported by the National Natural Science Foundation of China (NSFC) under grant numbers 51705163, the Fundamental Research Funds for the Central Universities(HUST) under grand numbers (2019JYCXJJ022, 2019kfyXKJC003), and the Unpowered Lower Extremity Exoskeleton System (COMAC-SFGS-2019-262).

Zefeng Yan, Haoyuan Yi, Zihao Du, Tiantian Huang and Bin Han are with State Key Laboratory of Digital Manufacturing Equipment and Technology, School of Mechanical Science and Engineering, Huazhong University of Science and Technology. (Bin Han is the corresponding author, binhan@hust.edu.cn).

Lufeng Zhang, Pengansi and Xinyu Wu are with CAS Key Laboratory of Human-Machine-Intelligence Synergic Systems, Shenzhen Institutes of Advanced Technology, Chinese Academy of Science. Guangdong Provincial Key Lab of Robotics and Intelligent System, Shenzhen Institutes of Advanced Technology, Chinese Academy of Sciences. (Xinyu Wu is also the corresponding author, xy.wu@siat.ac.cn)

Workers who engaged in such types work need to continuous handling for extended durations, which would cause their shoulder and elbow injures and serious occupational injures. Reducing the task load for these workers through the use of assistive exoskeleton could have a lot of benefits in term of the occupational life and the cost of these companies. For upper arm assistance, there are an increasingly large range of powered and passive exoskeleton products that aim to provide support for the humans' arm during different applies.

In recent decades, Various kinds of active and non-powered exoskeleton have been developed in universities and academies. Mao et al. [2],[3] designed a upper limb robot aimed at neural rehabilitation called CAREX. The shoulder motions are controlled by cables actuated through motor. The structure idea of exoskeleton is different form the traditional definition. That robot is proposed with on links and joints. Kiguchi et al. have developed a 7 DOF robot called SUEFUL-7 [4]. The designed device adapts the length between the shoulder joint of exoskeleton and the upper limb according to the user's shoulder joint motion. Perry et al. [5] have proposed anthropometric 7 DOF active exoskeleton, shown as EXO-7. The exoskeleton is suit the 95% human arm sizes. T.Nef et al. [6] [7] proposed a rehabilitation device, known as ARMin III, which can provide vertical motion because of the linear drive in the vertical direction. In addition to above translation, it also has the capacity to fit each patient by adjusting some adjustable links. Frisoli et al. [8] proposed an arm exoskeleton with 4 DOF named as L-EXOS. The exoskeleton can provide shoulder and elbow flexion/extension. It allows the wearer to put the exoskeleton on and take it off easily, without additional help of connecting upper limbs by a closed ring construction. Ruiz et al. [9] developed an active and wearable upper limb exoskeleton (WOTAS), which aimed at tremor assessment and suppression. The robot can provide assist at wrist joint and elbow. The WOTAS generate elbow flexion/extension, forearm pronation/supination and wrist flexion/extension by electric motors. X-arm-2 designed by ESA [10]. The robot consists of 8 active and 6 passive DOFs which is designed to moderate the noncoincidence of user's arm joints with the exoskeleton

joints. The 6-REXOS designed by [11] has 4 active and 2 passive DOFs included regmatic motions and rotational motions. The exoskeleton several measures to improve the physical human-robot interaction.

In this study, we propose a wearable upper limb exoskeleton to provide assist for workers who engaged in continuous manual handling task or people who full or partial loss of function of upper arm caused by accident injuries, myasthenia and stroke. The exoskeleton uses flexible rope driven by a DC motor to realize the shoulder and elbow joints linkage and uses ball screw to realize the self-locking in different positions in needed, which make the total weight of the prototype less than 2 kg and it convenient to carry. It does not hinder the activities of upper limb when the motor is turn off. We also assess the assistance efficiency by the comparison of IEMG of the upper-arm's muscular signals under four different loads before and after wearing the device.

The rest of this paper is organized as follows. Section II introduces the motions of upper limb, overall mechanical structure and dynamical model analysis. Section III describes the control method. We describe the test results and analyses in Section IV. The conclusion and future work are exhibited in Section V.

II. MECHANICAL STRUCTURE DESIGN

A. The Motions of Human Upper-limb

Fig. 1 briefly shows the main motions of the upper limb. The shoulder has three Degrees of Freedom (DOF), which includes shoulder flexion/ extension, shoulder abduction/adduction, and shoulder internal/external rotation. The elbow joint is consist of two jots: the humeroradial and humeroulnar. The elbow includes two DOF: elbow flexion/extension, elbow supination/pronation.

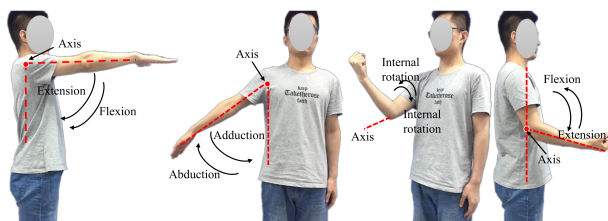


Fig. 1. The degrees freedom of the upper limb

B. Overall Mechanical Structure

The integral and partial structures of the upper limb exoskeleton are shown in Fig.2. It is composed of the shoulder module, elbow module and driver module. To simplify the structure and reduce the overall weight of the device, the wrist joint is not designed. The connection points between exoskeleton and human body

are consisting of elbow strap, shoulder strap and waist strap. If the motor of the deice is not turned on, the exoskeleton will not hinder the extension and flexion motions of the shoulder and elbow joints. This upper limb exoskeleton is able to realize the linkage of the shoulder and elbow joints by one small DC motor. It can be locked in a fixed position to assist the users' upper limb during the handling loads by the ball screw mechanism. This novel design of the structure can save energy, in the meantime, transfers the load to the exoskeleton, which will not give rise to the loss of the motor power.

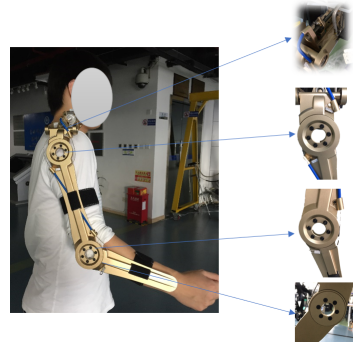


Fig. 2. The overall mechanical structure

The exoskeleton is connected with the wearers' upper limb by 3 straps, and the users need to take 30 seconds to put it on, meanwhile, only 20 seconds to take it off without additional assistance. The total weight of the overall system is 2 kg, which allows the user take it easily. The ergonomic structure design allows it is suitable for many associations. The shoulder and elbow have one flexion/extension freedom degree respectively, which can meet the demand of the daily handling task. The flexion/extension process of the exoskeleton are shown in Fig.3.

C. Dynamic Model Analysis

The human and exoskeleton coupling dynamic model shown in Fig.4. The system dynamic modeling uses the Euler Lagrange equation method [12]. m_1 is the mass of shoulder module of the exoskeleton and human body. r_1 is the length from the shoulder joint to center of mass. l_1 is the distance between the shoulder joint and the elbow joint. m_2 is the mass of the forearm of the human and exoskeleton, r_2 is length from the elbow joint to center of mass. The x-y coordinate system is established based on the cartesian coordinates.

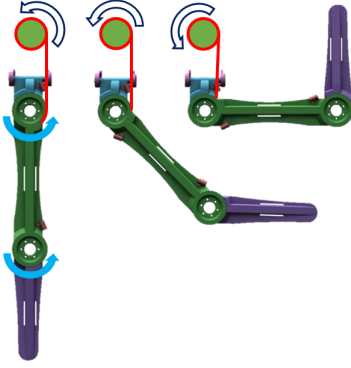


Fig. 3. The flexion/extension process of the exoskeleton

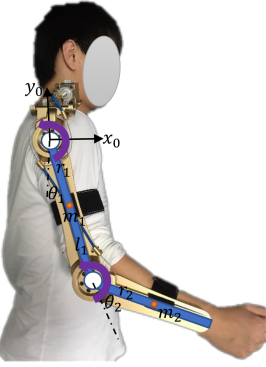


Fig. 4. The human-exoskeleton coupling dynamics model.

The vector of centroid position, velocity and angular velocity of shoulder are:

$${}_1^0\vec{P} = \begin{bmatrix} s_1 r_1 \\ -c_1 r_1 \\ 0 \end{bmatrix} \quad {}_1^0\vec{V} = \begin{bmatrix} c_1 r \\ s_1 r_1 \\ 0 \end{bmatrix} \quad {}_1^0\vec{\omega} = \begin{bmatrix} 0 \\ 0 \\ \dot{\theta}_1 \end{bmatrix} \quad (1)$$

The variable values of the fore arm are:

$${}_2^0\vec{P} = \begin{bmatrix} l_1 s_1 + r_2 s_{12} \\ -l_1 c_1 - r_2 c_{12} \\ 0 \end{bmatrix} \quad (2)$$

$${}_2^0\vec{V} = \begin{bmatrix} l_1 c_1 \dot{\theta}_1 + r_2 c_{12}(\dot{\theta}_1 + \dot{\theta}_2) \\ l_1 s_1 \dot{\theta}_1 + r_2 s_{12}(\dot{\theta}_1 + \dot{\theta}_2) \\ 0 \end{bmatrix} \quad {}_2^0\omega = \begin{bmatrix} 0 \\ 0 \\ \dot{\theta}_1 + \dot{\theta}_2 \end{bmatrix} \quad (3)$$

The kinetic energy E of the upper arm and fore arm are [13]:

$$E_1 = \frac{1}{2}m_1 {}_1^0\vec{V}^T {}_1^0\vec{V} + \frac{1}{2}I_1 {}_1^0\vec{\omega}^T {}_1^0\vec{\omega} = \frac{1}{2}m_1 r_1^2 \dot{\theta}_1^2 + \frac{1}{2}I_1 \dot{\theta}_1^2 \quad (4)$$

$$\begin{aligned} E_2 &= \frac{1}{2}m_2 {}_2^0\vec{V}^T {}_2^0\vec{V} + \frac{1}{2}I_2 {}_2^0\vec{\omega}^T {}_2^0\vec{\omega} \\ &= \frac{1}{2}m_2(l_1^2 \dot{\theta}_1^2 + r_2^2(\dot{\theta}_1 + \dot{\theta}_2)^2 + 2l_1 r_2 c_2(\dot{\theta}_1^2 + \dot{\theta}_1 \dot{\theta}_2)) \\ &\quad + \frac{1}{2}I_2(\dot{\theta}_1 + \dot{\theta}_2)^2 \end{aligned} \quad (5)$$

The total potential energy V of the system is:

$$V = -m_1 g r_1 \cos \theta_1 - m_2 g(l_1 \cos \theta_1 + r_2 \cos(\theta_1 + \theta_2)) \quad (6)$$

The kinetic energy E and the potential energy V are written as,

$$\begin{aligned} E &= \sum_{i=1}^2 \frac{1}{2}(m_i v_i^2 + J_i \dot{\theta}_i^2) \\ &= \frac{1}{2}J_{111}\dot{\theta}_1^2 + J_{12}\dot{\theta}_1\dot{\theta}_2 + \frac{1}{2}J_{22}\dot{\theta}_2^2 \\ V &= \sum_{i=1}^2 m_i g_i {}_i^0\vec{P}_y \end{aligned} \quad (7)$$

Formula (7) deduces θ_1 and θ_2 respectively:

$$\begin{aligned} \frac{\partial E}{\partial \theta_i} &= \frac{1}{2} \frac{\partial J_{11}}{\partial \theta_i} \dot{\theta}_1^2 + \frac{\partial J_{12}}{\partial \theta_i} \dot{\theta}_1 \dot{\theta}_2 + \frac{1}{2} \frac{\partial J_{22}}{\partial \theta_i} \dot{\theta}_2^2 \\ \frac{\partial E}{\partial \theta_i} &= J_{1i}\dot{\theta}_1 + J_{i2}\dot{\theta}_2 \quad (i = 1, 2) \end{aligned} \quad (8)$$

Substituting the above Formula (8) into the Lagrange equation:

$$\frac{d}{dt} \left(\frac{\partial E}{\partial \dot{\theta}_i} \right) - \frac{\partial E}{\partial \theta_i} + \frac{\partial V}{\partial \dot{\theta}_i} = \tau_i, \quad (9)$$

Bring Formula (9) represented as matrix form:

$$\begin{bmatrix} T_1 \\ T_2 \end{bmatrix} = \begin{bmatrix} m_1 r_1^2 + I_1 + m_2(l_1^2 + r_2^2 + l_1 r_2 c_2) + I_2 \\ m_2(r_2^2 + l_1 r_2 c_2) + I_2 \end{bmatrix} \begin{bmatrix} \ddot{\theta}_1 \\ \ddot{\theta}_2 \end{bmatrix} + \begin{bmatrix} m_2(r_2^2 + l_1 r_2 c_2) + I_2 \\ m_2 r_2 + I_2 \end{bmatrix} \begin{bmatrix} \ddot{\theta}_1 \\ \ddot{\theta}_2 \end{bmatrix} + \begin{bmatrix} 0 & -m_2 l_1 r_2 s_2 \\ m_2 l_1 r_2 s_2 & 0 \end{bmatrix} \begin{bmatrix} \dot{\theta}_1^2 \\ \dot{\theta}_2^2 \end{bmatrix} + \begin{bmatrix} -2m_2 l_1 r_2 s_2 & 0 \\ 0 & 2m_2 l_1 r_2 s_2 \end{bmatrix} \begin{bmatrix} \dot{\theta}_1 \dot{\theta}_2 \\ \dot{\theta}_2 \dot{\theta}_1 \end{bmatrix} + \begin{bmatrix} m_1 g r_1 s_1 + m_2 g l_1 s_1 + m_2 g r_2 s_{12} \\ m_2 g r_2 s_{12} \end{bmatrix} \quad (10)$$

III. CONTROL METHOD

The dynamic equation of the manipulator can be written as follows:

$$\tau = D(q)\ddot{q} + h_1(q, \dot{q}) + G(q) \quad (11)$$

To eliminate the steady-state position error, the value needs to be limited to a sliding surface,

$$\dot{\tilde{q}} + \Lambda \tilde{q} = 0 \quad (12)$$

Where Λ is a constant matrix. The desired trajectory is used as a constructed reference trajectory [14],

$$q_r = q_d - \Lambda \int_0^t \tilde{q} dt \quad (13)$$

$$\begin{aligned} \dot{q}_r &= \dot{q}_d - \Lambda \tilde{q}, & \ddot{q}_r &= \ddot{q}_d - \Lambda \dot{\tilde{q}} \\ s &= \tilde{q}_r = \dot{q} - \dot{q}_r = \dot{\tilde{q}} + \Lambda \tilde{q} \end{aligned} \quad (14)$$

Then the control law and the adaptive law are:

$$\begin{aligned} \tau &= \hat{D}(q)\ddot{q}_r + \hat{h}_1(q, \dot{q})\dot{q}_r + \hat{G}(q) - K_v s \\ \dot{a} &= -\Gamma^{-1}Y^T(q, \dot{q}, \dot{q}_r, \ddot{q}_r)s \end{aligned} \quad (15)$$

Now, the lyapunov function is used again to analyze the global stability of the tracking. Let the lyapunov function be [15]:

$$V(t) = \frac{s^T D s + \tilde{a}^T \Gamma \tilde{a}}{2} \quad (16)$$

The derivative with respect to $V(t)$,

$$\dot{V}(t) = -s^T K_v s \leq 0 \quad (17)$$

The above equation shows that the output error converges to the sliding plane,

$$s = \dot{\tilde{q}}_r = \dot{\tilde{q}} + \Lambda \tilde{q} = 0 \quad (18)$$

when $t \rightarrow \infty$, then $\tilde{q} \rightarrow 0$.

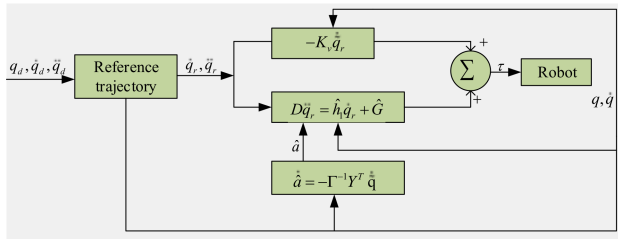


Fig. 5. The block diagram of the control

Fig.6 shows the two different planning trajectories and the average real trajectories. The motors complete planning trajectory based on PD adaptive control method. The experiment results demonstrate that control method is able to make sure the exoskeleton reach predetermined trajectory.

IV. EXPERIMENT

A. Participants

Five healthy subjects were volunteered to participate in sEMG signals acquisition. The height of these subjects ranged from 168cm to 183cm, and aged from 23 to 28 years old. These subjects had no previous upper limbs injuries.

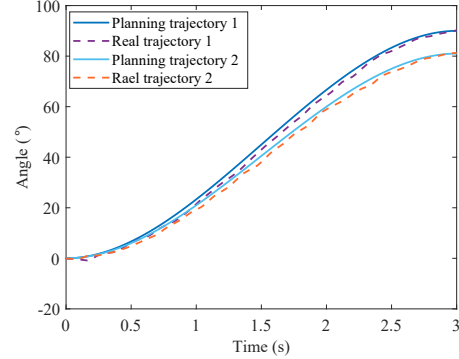


Fig. 6. The comparison between planning trajectory and real

B. Muscle Selection

Four muscles associated with shoulder and elbow joint activity were selected as follows: the deltoid muscle (DM), the biceps femoris muscle (BFM), the femoral muscle (FM), the femoral wrist flexor (FWF) as the muscles for collecting sEMG signals with and without the exoskeleton[16]. The position of the four muscles selected are show in Fig. 7(a). The position of the surface sEMG sensors are shown in Fig.7(b). To reduce impedance and external interference, the alcohol was used to clean and wipe the skin of the subjects before collecting the sEMG signal data.

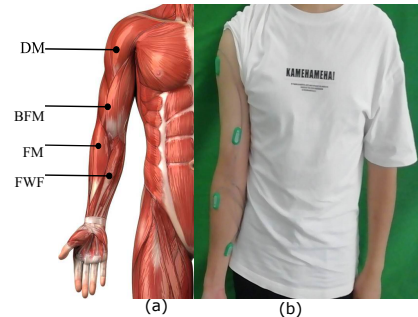


Fig. 7. (a) Four muscles, (b) The surface sEMG sensors

C. Testing Procedure

To validate a reduction of users' muscle activity achieved by the assist exoskeleton during handling task, the four muscle sEMG signals were measured in static handling task for four different loads (0, 1.5, 3.0, 4.5kg) with and without wearing the assist exoskeleton. Before beginning each test, the detailed trial procedures were ask to subjects, the exoskeleton's size was adjusted to suit the wearer's body size. The subjects were asked to maintain a static handling posture for 10 seconds under each loads. The muscle sEMG signals were measured five

times under each loads. Three different handling loads without exoskeleton are shown in Fig. 9.



Fig. 8. A subject static handling different loads with exoskeleton



Fig. 9. A subject static handling different loads without exoskeleton

D. Experimental Results and Analysis

Five healthy subjects were selected to participate in this trial. Shoulder and elbow muscle sEMG signals of the DM, BFM, FM and FWF were collected for four different loads (0,1.5,3.0,4.5 kg) before and after wearing the assist exoskeleton. The sEMG signals were filtered with a bandwidth of 10-100 HZ. Then the integral EMG values were calculated within a cycle. The assistance efficiency was defined:

$$E = 1 - \frac{I_e}{I}$$

where I_e is the IEMG when the upper limb bear objects with the assistance of EXO, I is the IEMG when upper limbs bear objects without assist exoskeleton.

Fig.10 - Fig.13 show the average IEMG of DM, BFM, FM and FWF for bearing 0 to 4.5kg loads respectively with and without the assist exoskeleton. It can be seen that the IEMG of same muscle increases with the weight of the objects. The IEMG values of the same muscle are almost equal when the load is 0kg before and after wearing the exoskeleton. The IEMG of every muscle is significantly decreased when the user wears the exoskeleton. The assistance effectively is different between the four muscles under same loads. When wearing the assist exoskeleton handling the objects from 1.5kg to 4.5kg, the IEMG reduction ranged from 35.4% to 45.6% for the DM, the reduction ranged from 36.2% to 47.1% for BFM, the reduction ranged from 33.4% to 41.0% for FM and the reduction ranged from 36.4% to 43.7% for FWF respectively. The average assistance efficiency were 39.1%, 41.5%, 36.5% and 40.6% for the DM, BFM, FM and FWF respectively. The experimental data demonstrate the upper limb exoskeleton is able to reduce muscular activity when wearing the exoskeleton for handling same objects. It can assist worker reduce the muscle fatigue during long-term handling work.

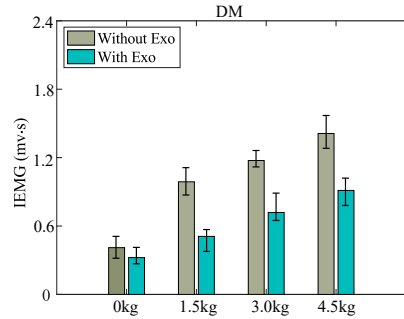


Fig. 10. IEMG of DM when bearing 0-4.5kg objects with and without exoskeleton

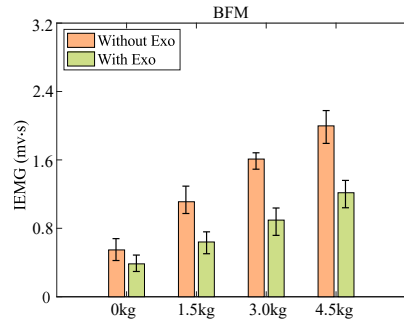


Fig. 11. IEMG of BFM when bearing 0-4.5kg objects with and without exoskeleton

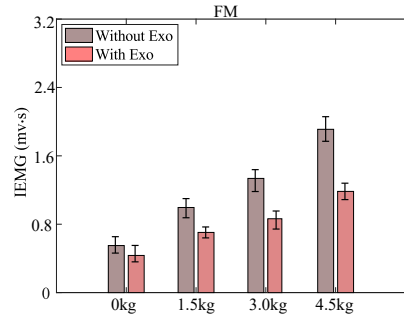


Fig. 12. IEMG of FM when bearing 0-4.5kg objects with and without exoskeleton

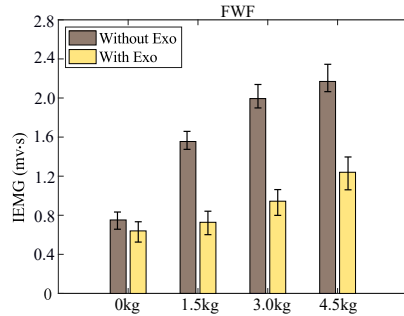


Fig. 13. IEMG of FWF when bearing 0-4.5kg objects with and without exoskeleton

V. CONCLUSIONS

In this paper, We describe the design of a wearable upper arm exoskeleton to provide support for industrial workers who engaged in repetitive handling tasks and patients who full or partial loss of function in their upper limb due to accident injuries, spinal cord and strokes. The assessment of the assistance effects of upper limb exoskeleton to reduce muscular activity was also described in this study. The total weight of the prototype is only 2 kg. We use one motor to realize the shoulder and elbow joints linkage and the self-locking in any position, this novel design make it convenient to employ in different occasions. The PD adaptive control method is applied to the proposed exoskeleton to track expected trajectories based on human-exoskeleton coupling dynamic model. Upper limb muscle signals of the deltoid muscle(DM), the biceps femoris muscle (BFM), the femoral muscle (FM), the femoral wrist flexor (FWF) were compared in continuous handling for four different loads (0, 1.5, 3, 4.5kg) before and after wearing the assist exoskeleton. The average assistance efficiency were 39.1%, 41.5%, 36.5% and 40.6% for the DM, BFM, FM and FWF respectively. The experimental data show that the upper limb exoskeleton significantly reduce IEMG values during conscious handling loads.

There is still a lot of work to be done in the future. First of all, the mechanical structures need to increase more degrees of freedom, such as shoulder abduction/adduction, shoulder internal/external rotation and the elbow supination/pronation. The more lightweight material and higher power density motor should be used to the prototype to reduce the total weight. Second, we will study the understanding of the human upper limb movement intention based on EEG signals or EMG signals and study the interaction between exoskeleton and human' upper limb to make it more adaptive in the next work.

Acknowledgment

We would like to tank Shengcai Duan and Hao Ren for their contributions in this experiment, Xu Yong and Cao Wang for their contributions in the exoskeleton.

References

- [1] R. Gopura, D. Bandara, K. Kiguchi, and G. K. Mann, "Developments in hardware systems of active upper-limb exoskeleton robots: A review," *Robotics and Autonomous Systems*, vol. 75, pp. 203–220, 2016.
- [2] Y. Mao and S. K. Agrawal, "Design of a cable-driven arm exoskeleton (carex) for neural rehabilitation," *IEEE Transactions on Robotics*, vol. 28, no. 4, pp. 922–931, 2012.
- [3] Y. Mao and S. K. Agrawal, "Transition from mechanical arm to human arm with carex: A cable driven arm exoskeleton (carex) for neural rehabilitation," in 2012 IEEE International Conference on Robotics and Automation, pp. 2457–2462, IEEE, 2012.
- [4] R. A. R. C. Gopura, K. Kiguchi, and Y. Li, "Sueful-7: A 7dof upper-limb exoskeleton robot with muscle-model-oriented emg-based control," in 2009 IEEE/RSJ International Conference on Intelligent Robots and Systems, pp. 1126–1131, IEEE, 2009.
- [5] J. C. Perry, J. Rosen, and S. Burns, "Upper-limb powered exoskeleton design," *IEEE/ASME transactions on mechatronics*, vol. 12, no. 4, pp. 408–417, 2007.
- [6] M. Mihelj, T. Nef, and R. Riener, "Armin ii-7 dof rehabilitation robot: mechanics and kinematics," in Proceedings 2007 IEEE International Conference on Robotics and Automation, pp. 4120–4125, IEEE, 2007.
- [7] T. Nef, M. Guidali, and R. Riener, "Armin iii-arm therapy exoskeleton with an ergonomic shoulder actuation," *Applied Bionics and Biomechanics*, vol. 6, no. 2, pp. 127–142, 2009.
- [8] A. Frisoli, F. Rocchi, S. Marcheschi, A. Dettori, F. Salsedo, and M. Bergamasco, "A new force-feedback arm exoskeleton for haptic interaction in virtual environments," in First Joint Eurohaptics Conference and Symposium on Haptic Interfaces for Virtual Environment and Teleoperator Systems. World Haptics Conference, pp. 195–201, IEEE, 2005.
- [9] A. Ruiz, A. Forner-Cordero, E. Rocon, and J. L. Pons, "Exoskeletons for rehabilitation and motor control," in The First IEEE/RAS-EMBS International Conference on Biomedical Robotics and Biomechatronics, 2006. BioRob 2006., pp. 601–606, IEEE, 2006.
- [10] A. Schiele and G. Hirzinger, "A new generation of ergonomic exoskeletons-the high-performance x-arm-2 for space robotics telepresence," in 2011 IEEE/RSJ International Conference on Intelligent Robots and Systems, pp. 2158–2165, IEEE, 2011.
- [11] M. Gunasekara, R. Gopura, T. Jayawardena, and G. I. Mann, "Dexterity measure of upper limb exoskeleton robot with improved redundancy," in 2013 IEEE 8th International Conference on Industrial and Information Systems, pp. 548–553, IEEE, 2013.
- [12] Z. Li, Z. Huang, W. He, and C.-Y. Su, "Adaptive impedance control for an upper limb robotic exoskeleton using biological signals," *IEEE Transactions on Industrial Electronics*, vol. 64, no. 2, pp. 1664–1674, 2016.
- [13] M. H. Rahman, M. J. Rahman, O. Cristobal, M. Saad, J.-P. Kenné, and P. S. Archambault, "Development of a whole arm wearable robotic exoskeleton for rehabilitation and to assist upper limb movements," *Robotica*, vol. 33, no. 1, pp. 19–39, 2015.
- [14] R. Lu, Z. Li, C.-Y. Su, and A. Xue, "Development and learning control of a human limb with a rehabilitation exoskeleton," *IEEE Transactions on Industrial Electronics*, vol. 61, no. 7, pp. 3776–3785, 2013.
- [15] E. Burdet, G. Ganesh, C. Yang, and A. Albu-Schäffer, "Interaction force, impedance and trajectory adaptation: by humans, for robots," in *Experimental Robotics*, pp. 331–345, Springer, 2014.
- [16] K. Huysamen, T. Bosch, M. de Looze, K. S. Stadler, E. Graf, and L. W. O'Sullivan, "Evaluation of a passive exoskeleton for static upper limb activities," *Applied ergonomics*, vol. 70, pp. 148–155, 2018.